Wavelength selection of fingering instability inside Hele–Shaw cells

J. Fernandez, P. Kurowski, L. Limat, and P. Petitjeans
Laboratoire de Physique et Mécanique des Milieux Hétérogènes, CNRS,
Ecole Supérieure de Physique et de Chimie Industrielles, 10 rue Vauquelin, 75005 Paris, France

(Received 19 March 2001; accepted 20 July 2001)

Fingering instabilities involving fluids confined between two plates sometimes give rise to a typical wavelength λ proportional to the gap h. This unexplained behavior is investigated for the case of the Rayleigh–Taylor instability between two liquids of the same viscosity. Using qualitative scaling arguments and linear stability analysis for a simplified model of hydrodynamics, we show that, in the miscible case, h becomes a natural cut-off when diffusion is negligible, i.e., when the Péclet number $\mathrm{Pe}=h^3\Delta\rho g/(\eta D)$ is large (η viscosity, g gravitational acceleration, D diffusivity, $\Delta\rho$ density difference). The same result holds in the immiscible case for large capillary number $\mathrm{Ca}=h^2\Delta\rho g/(12\gamma)$ (γ surface tension). In this saturation regime, the dominant wavelength is given by $\lambda\approx 2.3h$, while in the opposite limit (low Pe or low Ca) λ scales, respectively, as h/Pe or $h/\mathrm{Ca}^{1/2}$. These results are in agreement with a recent experimental study. © *2001 American Institute of Physics.* [DOI: 10.1063/1.1410120]

I. INTRODUCTION

The instabilities of an interface between miscible or immiscible fluids induced by differences in viscosity or density have stimulated growing interest[1,2] motivated by numerous applications (pharmacology and chemical industries,[3–5] geophysics,[6–9] etc.). In this paper, we consider the case of two fluids in a Hele–Shaw cell, which constitutes a rough but simple representation of a porous material. Indeed, many applications, such as oil recovery, take place in such a medium. Available studies have identified different cases, which depend on the nature of the instability (viscous or gravitational), and on the ratio of advection to molecular diffusion or surface tension effects, usually measured, depending on whether or not the fluids are miscible, either by a Péclet number or a capillary number, both dimensionless. Viscous instability is generally referred to as Saffman–Taylor instability, and Rayleigh–Taylor is generally associated with gravity-driven instability, although it should be pointed that Saffman and Taylor in their seminal paper[10] included both pressure-driven and gravity-driven cases in the high friction limit (low-Reynolds) which corresponds to the Hele–Shaw flow. For low Péclet or low capillary number, i.e., when diffusion or surface tension dominates, the typical wavelength λ is a function of the diffusivity or surface tension,[1,11,12] while in the opposite limit, experiments[13–15] reveal that its value, normalized by the cell thickness h, saturates at a constant value. Available theoretical models have mostly discussed the first regime, but no satisfactory explanation has been proposed for the behavior of the wavelength at high values of the Péclet or capillary number. A tentative explanation was suggested by Patterson[15] in the case of miscible fluids, but it is based upon a principle of minimum dissipation which, to our knowledge, still remains unproven.

In this paper, we reconsider this problem in the simplest possible situation, a Rayleigh–Taylor instability[16,17] induced by a density mismatch between two fluids of equal viscosity, at very low Reynolds number. We propose a new explanation for the saturation regime by using simple qualitative arguments (Sec. II), and we check our interpretation on a simplified version of the equations governing fluid motion (Sec. III). In short, we replace the Stokes equation by an effective equation for the mean velocity averaged over the cell gap, in which the derivatives in the direction normal to the plate are deduced from an ideal Poiseuille flow, similar to that involved in the Darcy regime. Sometimes called a ''Brinkman'' model in the literature related to porous media, this model allows us to obtain both limits, i.e., a Darcy flow interacting with diffusion at low Péclet number or surface tension at low capillary number, and a Stokes flow at high Pe or high Ca. In the miscible case, the results are compared to recent experimental measurements.[18] Very good agreement is found for a wide range of Péclet numbers (from 0.1 to 10^4).

II. PHENOMENOLOGICAL APPROACH

A. Qualitative argument

The geometry of the problem is suggested in Fig. 1. A fluid of density ρ_1 tests on top of a lighter one of density $\rho_2=\rho_1-\Delta\rho$, both fluids being confined between two vertical plates separated by a gap h. Usually, the stability of an interface is discussed by calculating a dispersion relation $\sigma(k=2\pi/\lambda)$ that governs the growth of initial sinusoidal perturbations of the interface position $\delta z\propto\exp(ikx+\sigma t)$, where k is assumed to be positive in this section. Neglecting for the moment any damping effect associated with diffusion or surface tension, and restricting the analysis to low Reynolds number (where inertial effects are negligible), this dispersion relation should correspond to an equilibrium between buoyancy effects and viscous stresses. Without going into the details of the calculations, we can estimate the scaling involved as follows.

At the beginning of its growth, a ''finger'' or a ''cell'' of

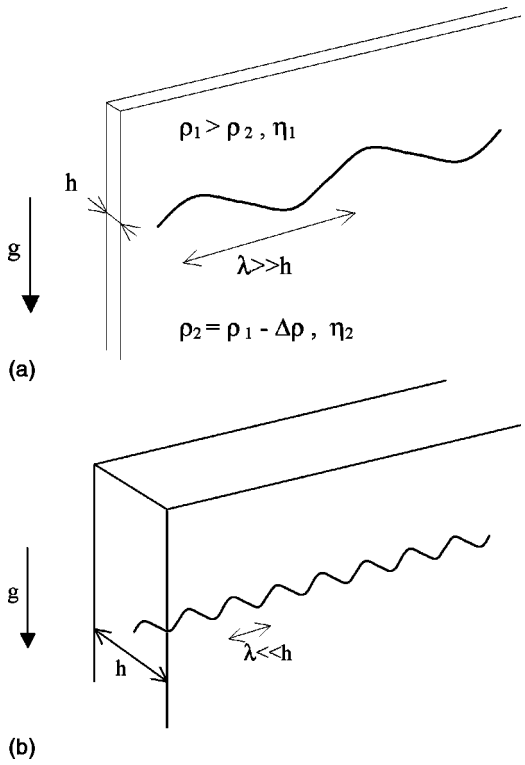

FIG. 1. (a) Schematic representation of the interfacial instability. The upper and the lower layer have, respectively, density ρ_1 and density $\rho_2=\rho_1+\Delta\rho$. In the Darcy regime ($\lambda \gg h$), the friction exerted on the patterns interacts with the plates of the cell across a surface area of order λ^2. As a result, the global buoyancy force $F_B=(h\lambda\zeta)g\Delta\rho$ is counterbalanced by the viscous force $F_V=\eta\lambda^2(\sigma\zeta/h)$. (b) Schematic representation of the interface in the Stokes regime ($\lambda \ll h$). The friction exerted on a finger occurs on a scale that is now the pattern wavelength. Thus, the buoyancy force F_B is counterbalanced by the viscous force $F_V=\eta(\lambda h)(\sigma\zeta/h)$.

the pattern, typically of size $\lambda/2$ in the x direction, is subjected to a global buoyancy force or order $F_B \propto (h\lambda\varsigma)g\Delta\rho$ where ς designates the pattern amplitude. This force is balanced by a force of viscous origin of a form depending on the range of wavelengths considered [see Figs. 1(a) and 1(b)]. When $\lambda \gg h$, we are in a Darcy regime, in which most of the viscous friction acting on the cell will be interacting with the solid boundaries, over a surface area typically of order λ^2 (λ is also the characteristic extent of the flow in the z direction). We thus expect the viscous force to scale as $F_V \propto \eta\lambda^2(\sigma\zeta/h)$ where η is the viscosity, and $\sigma\zeta/h$ a typical velocity gradient. In the opposite limit $\lambda \ll h$, the typical gradient becomes $\sigma\zeta/\lambda$ and the typical surface area λh, the viscous force acting mainly between lateral cells. The viscous force now scales as $F_V \propto \eta(\lambda h)(\sigma\zeta/\lambda)$. The dispersion relation is deduced, at least qualitatively, by writing the equality $F_B=F_V$. To get an idea of the influence of diffusion or surface tension, we can also introduce in the result a phenomenological damping term $-A$. This leads to

$$\sigma=-A+\frac{h^2}{\eta}g\Delta\rho k \quad (k \ll 1/h), \tag{1a}$$

$$\sigma=-A+\frac{g\Delta\rho}{\eta k} \quad (k \gg 1/h), \tag{1b}$$

where $A \propto Dk^2$ in the miscible case, and $A \propto (\gamma h^2/\eta)k^3$ in the immiscible case.[1]

Of course, as we shall see, the actual relationship has a more complicated algebraic structure and involves numerical prefactors omitted here. However, Eq. (1) is sufficient to lead to the following predictions. At very low k, one recovers qualitatively the well-known Darcy type dispersion relation: $\sigma=(h^2/24\eta)\Delta\rho\, g\, k$,[19] which favors the growth of small wavelengths.

The Péclet number is defined here as $\mathrm{Pe}=U^*h/D$ with a characteristic velocity of finger growth $U^*=\Delta\rho g h^2/12\eta$. Similarly the capillary number is $\mathrm{Ca}=\eta U^*/\gamma$. As it appears from Eq. (1), when the Péclet or the capillary number is large enough, diffusion or surface tension becomes insignificant and the wavelength selection should result solely from a crossover from the Darcy regime to a ''Stokes regime'' in which σ decreases with k (regime $k \gg 1/h$). In this case, i.e., for $\mathrm{Pe} \gg 1$ or for $\mathrm{Ca} \gg 1$, the most unstable wavelength $\lambda_{\max}$ should be proportional to the gap, i.e., $\lambda_{\max} \sim h$. In the opposite limit, the crossover to a diffusion- or surface-tension-limited growth will occur before k reaches $1/h$, so that the dominant wavelength scales as $\lambda_{\max} \sim h/\mathrm{Pe}$ in the miscible case, or $\lambda_{\max} \sim h/\mathrm{Ca}^{1/2}$ in the immiscible case.

B. Physical interpretation of the result

From a physical point of view, the saturation of the wavelength at high Pe or high Ca has its origin in a change of the mechanisms which govern the viscous effects, as opposed to the growth. In the Darcy limit (large wavelength), most of the friction exerted on a finger interacts directly with the plates [Fig. 1(a)], over a length scale which coincides with the gap h. In the Stokes limit (small wavelength), most of the friction occurs laterally against the reversed flow induced around neighboring fingers, on a scale that is now the pattern wavelength [Fig. 1(b)]. The scale h emerges as a compromise between these two limits. At low Pe or Ca, this mechanism is hidden by a more conventional crossover between Darcy-limited growth and diffusion or surface tension.

III. LINEAR STABILITY ANALYSIS

A. Approximating Stokes equations with a Brinkman model

We now describe more precisely the hydrodynamics involved, again at very low Reynolds number. In this limit, both liquids follow Stokes law, but the resulting equations are still difficult to solve.[20] We have therefore replaced this problem by a simpler one, writing approximate equations for the mean velocity averaged, over the cell thickness:

$$\mathbf{0}=-\boldsymbol{\nabla}P+\eta\left[\frac{12}{h^2}+\boldsymbol{\nabla}^2\right]\mathbf{U}+\rho\mathbf{g}, \tag{2a}$$

$$\mathbf{0}=\boldsymbol{\nabla}\cdot\mathbf{U}, \tag{2b}$$

where $P(x,z,t)$ and $\rho(x,z,t)$ are, respectively, the pressure and density fields, $\mathbf{U}=(U_x,U_z)$ is the fluid velocity averaged over the cell thickness, and the operator $\boldsymbol{\nabla}=(\partial_x,\partial_z)$ is de-

fined for coordinates x and z only. These equations are sometimes called a Brinkman model[21] in the literature related to porous media.

B. Miscible case

Equations (2a) and (2b) must be coupled with a diffusion equation:

$$\rho=\rho_2+(\rho_1-\rho_2)c, \tag{3a}$$

$$\frac{\partial c}{\partial t}+(\mathbf{U}\cdot\boldsymbol{\nabla})c=D\boldsymbol{\nabla}^2 c, \tag{3b}$$

where $c(x,z,t)$ is the local concentration of liquid 1. The density difference $\Delta\rho=\rho_1-\rho_2$ is assumed small compared to ρ_1, which allows the linearization of the (ρ,c) relation (3a). It should be noted that (2a) will reduce to Darcy's equation in the limit $\lambda\ll h$, and to a Stokes flow in the opposite limit $\lambda\gg h$, in agreement with the qualitative ideas discussed at the beginning of this paper.

1. Base state and its perturbations

For a flat interface, initially perfect, with a discontinuous concentration profile, the system is expected to evolve solely by diffusion. It should remain in a time-dependent base state with zero velocity $\mathbf{U}_0=\mathbf{0}$, and a hydrostatic pressure field $P_0(x,z,t)$ governed by the evolution of the concentration $c(x,z,t)$ according to

$$\boldsymbol{\nabla}P_0=[\rho_2+\Delta\rho c_0(z,t)]\mathbf{g}, \tag{4a}$$

$$c_0(z,t)=\tfrac{1}{2}[1+\mathrm{erf}(z/\sqrt{Dt})] \tag{4b}$$

in which $\mathrm{erf}(u)$ designates the error function. In the *real* case of an interface initially slightly perturbed, one should include perturbation terms, i.e., $\mathbf{U}=\mathbf{0}+\mathbf{u}(x,z,t)$, $P(x,z,t)=P_0(z,t)+p(x,z,t)$, and $c(x,z,t)=c_0(z,t)+c'(x,z,t)$. Linearizing the equations, we get the following two equations that couple the concentration perturbation $c'(x,z,t)$ to the z-component of the perturbation velocity $u_z(x,z,t)$:

$$\eta\nabla^2\left[\frac{12}{h^2}-\nabla^2\right]u_z=-\Delta\rho g\frac{\partial^2 c'}{\partial x^2}, \tag{5a}$$

$$\left[\frac{\partial}{\partial t}-D\nabla^2\right]c'=-\frac{\partial c_0}{\partial z}u_z. \tag{5b}$$

Following a method previously applied by Kurowski and Misbah[22] to unconfined Rayleigh–Taylor instabilities, we expand now u_z and c' into normal modes, $[u_z,c']=[w_1(z),c_1(z)]\exp(ikx+\sigma t)$, where σ is supposed to be defined at very small time in a quasisteady state approximation. As long as time remains much smaller than the diffusion time scale, we assume a sharp profile for the diffusion field: $\partial c_0/\partial z=\delta(z)$, $\delta(z)$ being the Dirac delta function. This yields a single differential equation for w_1:

$$\left[\frac{d^2}{dz^2}-k^2\right]\left[\frac{12}{h^2}-\frac{d^2}{dz^2}+k^2\right]\left[\sigma-D\left(\frac{d^2}{dz^2}-k^2\right)\right]w_1$$
$$=-\frac{g\Delta\rho}{\eta}k^2\delta(z). \tag{6}$$

For $z=0$, δ vanishes, and w_1 can be expressed as a linear combination of the functions $\exp(\pm kx)$, $\exp(\pm 1x)$, and $\exp(\pm\xi x)$, with $l^2=k^2+\sigma/D$ and $\xi^2=k^2+12/h^2$. The coefficients, which are different in the two half spaces $z>0$ and $z<0$, are linked by the continuity of w_1 across the interface $(z=0)$, that of its derivatives up to the fifth order in d/dz and a discontinuity condition in the sixth-order derivative deduced from Eq. (6) (see Ref. 23 for more details). Elimination of these coefficients leads to the dispersion relation discussed in the following.

2. Dispersion relation: From low to large Péclet numbers

After some cumbersome algebra, we finally obtain the following dispersion relation that links the reduced growth rate $\Sigma=12\eta\sigma/\Delta\rho g h$ to the reduced wave vector $q=|k|h$, both quantities being here rendered dimensionless by using the scaling factors identified qualitatively at high Péclet number in Sec. II:

$$\Sigma=\frac{12}{\mathrm{Pe}}+\frac{q}{2}\left[1-\frac{q}{\sqrt{12+q^2}}\right]-\frac{6q}{\mathrm{Pe}\,\Sigma}\left[1-\frac{q}{\sqrt{\mathrm{Pe}\,\Sigma+q^2}}\right]. \tag{7}$$

The implicit equation (7), which can be reduced to a fourth-order polynomial, is solved numerically for a large range of Péclet numbers. We show an example of these four solutions for $\mathrm{Pe}=10^3$ in Fig. 2: The real and the imaginary parts of the reduced growth rate Σ are represented in Figs. 2(a) and 2(b), respectively. The branch Σ_1 is always real and displays a maximum. The two branches Σ_2 and Σ_3 are real up to $q=5.65$ and then become complex conjugates. These two solutions are not relevant in this case. The fourth solution Σ_4 remains constant and positive $\Sigma_4=12/\mathrm{Pe}$. This branch Σ_4 represents the characteristic diffusion time across the gap in the cell, $\tau_D=K/D$ ($K=h^2/12$, where K is the permeability of the cell). The dispersion relation which corresponds to Σ_1 is displayed in Fig. 3 for four different values of Pe (1, 10, 10^2, and 10^4). The wave vector $q_{\max}$ corresponding to the maximum growth rate $\Sigma_{\max}$ increases with Pe until it saturates at $q_{\mathrm{sat}}=2.7$ (i.e., $\lambda/h=2.3$)for high Pe ($\mathrm{Pe}>100$). This value corresponds to the most unstable wave vector obtained from the dispersion relation, Eq. (7), in the asymptotic case ($\mathrm{Pe}\to\infty$):

$$\Sigma_{\mathrm{Pe}\to\infty}=\frac{q}{2}\left[1-\frac{q}{\sqrt{12+q^2}}\right]. \tag{8}$$

Note that although $q_{\max}$ tends to a constant value with increasing Pe, the cutoff wave vector $q_c[\Sigma(q_c)=0]$ continues to increase. Indeed, the larger Pe, the smaller the diffusion length becomes, so that larger q become unstable. This behavior, i.e., the saturation of $q_{\max}$ coupled to the increase of q_c has also been noted by Brown[24] for the Rayleigh–Taylor instability of a thin viscous layer between immiscible fluids.

The most unstable wavelength, normalized by the gap, $\lambda_{\max}/h=2\pi/q_{\max}$ and the growth rate $\Sigma_{\max}$, are represented as functions of Pe in Fig. 4. For large values of Pe, the wavelength scales with the gap of the cell, $\lambda_{\max}=2.3h$ and

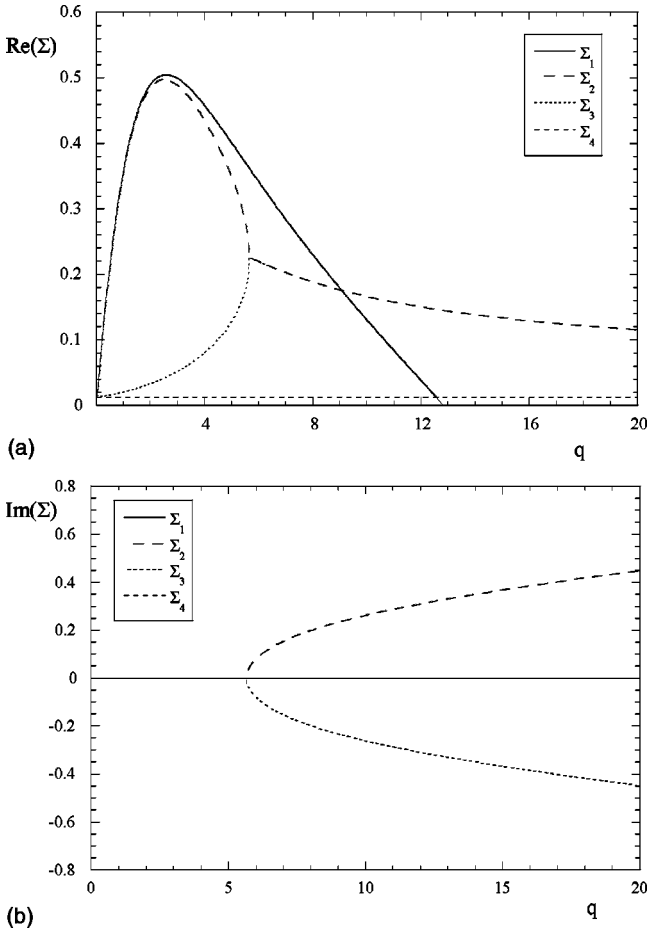

FIG. 2. Solutions of the dispersion relation, Eq. (7), at $\mathrm{Pe}=10^3$. (a) Real part of Σ vs q. (b) Imaginary part of Σ vs q.

the growth rate is constant, $\Sigma_{\max}=0.4$. This is the main result derived from this model. Moreover, the dispersion relation (7) covers both the diffusive regime at low Pe (Darcy's regime) and the convective regime at large Pe (Stokes regime).

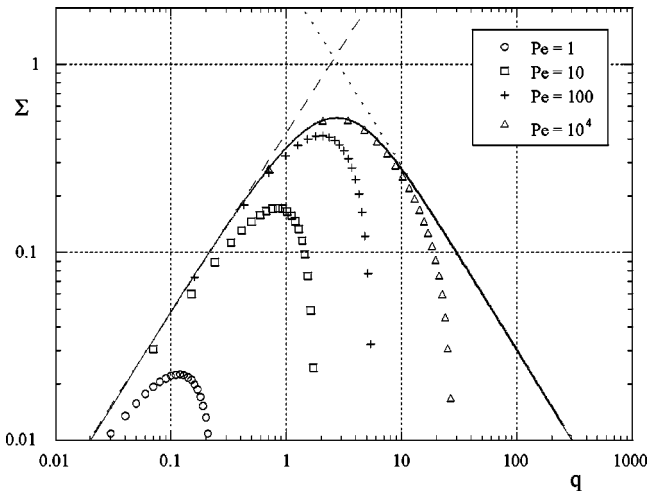

FIG. 3. Growth rate Σ_1 as a function of the wave vector q for Pe = 1, 10, 10^2, and 10^4. The continuous line represents the asymptotic ($\mathrm{Pe}\to\infty$) dispersion relation. The dashed line corresponds to the asymptotic behavior in the Darcy regime ($\Sigma=q/2$), and the dotted line represents the asymptotic behavior in the Stokes regime ($\Sigma=3/q$). The crossover between these two asymptotic regimes yields a wavelength proportional to the thickness of the cell.

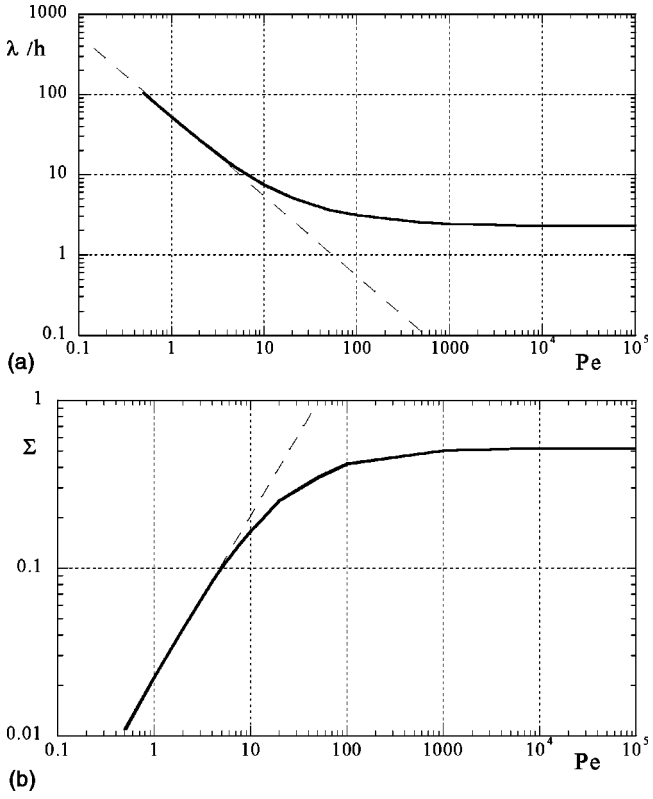

FIG. 4. (a) λ/h vs Pe. At low Pe, the dimensionless wavelength scales as Pe^{-1}, and is equal to 2.3 at large Pe. (b) $\Sigma_{\max}$ vs Pe. At low Pe (Darcy regime), Σ scales as Pe, and it is equal to 0.4 at large Pe (Stokes regimes).

The agreement between these theoretical values of $\lambda_{\max}$ and $\Sigma_{\max}$ with recent experiments, as well as with numerical simulations, is very good,[18] notably when the Reynolds number is very low. In particular, the asymptotic wavelength observed by Fernandez *et al.*[18] was closer to the theoretical value (2.3 h) for larger viscosity (smaller Re) than for lower viscosity flow (lower Re). Indeed, when the Reynolds number is not negligible, the assumption of a parabolic profile in the gap is no longer valid.

In the limit $\mathrm{Pe}\ll 1$, Eq. (7) reduces to the characteristic dispersion relation of the Darcy's regime:[1,12]

$$\Sigma=\frac{1}{2}(q-\mathrm{Pe}^{-1}\,q^2-\mathrm{Pe}^{-1}\,q\sqrt{q^2+2\,\mathrm{Pe}\,q}). \tag{9}$$

The most unstable modes $\lambda_{\max}/h$ and $\Sigma_{\max}$ calculated from Eq. (9) scale, respectively, as Pe^{-1} and as Pe.

The change of behavior between low and large Péclet numbers and the selection of the wavelength, can be pointed out qualitatively by intersecting the two qualitative equations (1a) and (1b). This leads to $\lambda/h=2\pi$, which is an approximation not so far from the theoretical value 2.3.

C. Immiscible case

We now apply the Brinkman model to an interface between two immiscible fluids of the same viscosity, in the same geometry. At $t=0$ the interface ($z=\zeta_0=0$) is slightly disturbed. $\zeta'(x,z,t)$, $\mathbf{U}'$, $\rho'(x,z,t)$, and p' represent the perturbation field. The linearized equations for the perturbations read

$$0 = -\nabla p' + \eta\left[\frac{12}{h^2} + \nabla^2\right]\mathbf{U}' + \rho'\mathbf{g} + \frac{\pi}{4}\gamma\frac{\partial^2\zeta'}{\partial z^2}\delta(z-\zeta_0), \tag{10a}$$

$$0 = \nabla\cdot\mathbf{U}', \tag{10b}$$

where

$$\gamma\frac{\partial^2\zeta'}{\partial z^2}\delta(z-\zeta_0)$$

represents the discontinuity of the pressure at the interface and $\delta(z)$ is the Dirac delta function. This expression is not trivial but is consistent with the analysis of Park and Homsy[25] after neglecting the pressure gradient in the cell gap due to the transverse meniscus.[26] These equations must be coupled with the linearized incompressibility condition:

$$\frac{\partial\rho'}{\partial t} + w\frac{\partial\rho}{\partial z} = 0. \tag{11}$$

Expanding the perturbations into normal modes $\exp(ikx+\sigma t)$, and taking into account that $d\zeta'/dt = w'(\zeta') = \sigma\zeta'$ where $w'(\zeta')$ is the vertical velocity of the interface $z=\zeta'(x,z,t)$, yields a single differential equation for the amplitude w_1 of w:

$$\eta\sigma\left[\frac{\partial}{\partial z^2} - k^2 - \frac{12}{h^2}\right]\left[\frac{\partial}{\partial z^2} - k^2\right]w_1$$

$$= -g\Delta\rho k^2\delta(z)w_1 + \gamma k^4\delta(z)w_1 - \Delta\rho\sigma^2\delta(z)\frac{\partial w_1}{\partial z}. \tag{12}$$

For $z=0$, δ vanishes and w_1 can be expressed as a linear combination of the functions $\exp(\pm ikx)$, $\exp(\pm ilx)$ with $l^2 = k^2 + 12/h^2$. The coefficients, which differ in the two half spaces $z>0$ and $z<0$, are matched as a result of the continuity of the velocity and the tangential stress across the interface ($z=0$). Thus, integrating Eq. (12) over an infinitesimal layer of thickness ε ($\varepsilon\to 0$) which includes the interface between the two fluids, the dispersion relation is obtained:

$$2\eta\frac{12}{h^2}\sigma = |k|(g\Delta\rho - \gamma k^2)\left[1 - |k|\left(k^2 + \frac{12}{h^2}\right)^{-1/2}\right]. \tag{13}$$

The wavelength corresponding to the maximum growth rate is plotted, together with the miscible case, in Fig. 5 as a function of the capillary number.

Using the reduced growth rate $\Sigma = 12\eta\sigma/g\Delta\rho h$ and the reduced wave vector $q = |k|h$ with the capillary number Ca, the dispersion relation [Eq. (13)] reduces to

$$\Sigma = \frac{1}{2}\left(q - \frac{q^3}{12\ \mathrm{Ca}}\right)\left(1 - \frac{q}{\sqrt{q^2+12}}\right). \tag{14}$$

At low Ca ($q \ll 1$), the most unstable wavelength λ/h scales as $\mathrm{Ca}^{-1/2}$.[1,19] At large Ca, Eq. (14) yields the same asymptotic dispersion relation as the miscible one—Eq. (8). The most unstable wavelength λ/h is also constant: $\lambda/h = 2.3$, just as for the miscible case. Experimentally this behavior has been observed by Maxworthy[27] and Maher[28] with, however, a different asymptotic value (respectively, $\lambda/h \sim 5$ and $\lambda/h \sim 3$).

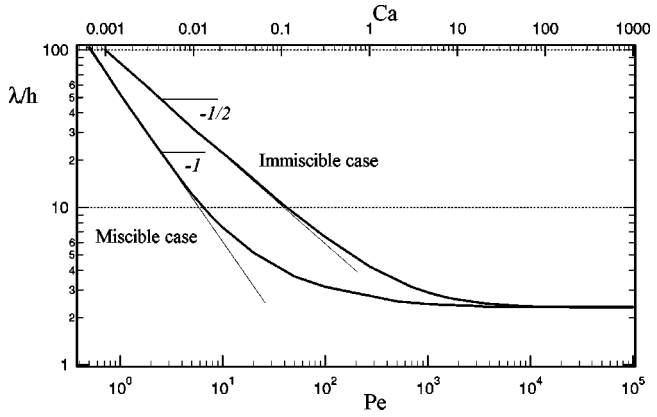

FIG. 5. Evolution of the reduced wavelength λ/h as a function of the capillary number Ca. The miscible case has been overlaid in order to show that the asymptotic limits are the same.

IV. CONCLUSION

A complete dispersion relation has been obtained for the instabilities between miscible fluids as well as for immiscible fluids. These equations cover the whole range of parameters from the Darcy regime to the Stokes regime. This has been achieved using a Brinkman equation instead of a Darcy model. Comparison with experiments is very good.[18] Moreover, numerous papers[29,30] have reported the observation of the asymptotic behavior that can be explained by the model presented in this paper. In the near future, this dispersion relation will be extended to the case of miscible, or immiscible, fluids with different densities, viscosities, and velocities. A further interesting challenge would be to study the transition from a Hele–Shaw geometry toward a three-dimensional configuration.

Moreover, we have observed that the instabilities between miscible or immiscible fluids have the same asymptotic behavior ($\lambda = 2.3h$) in the convective regime: miscible fluids at large Péclet number, i.e., when the diffusion is negligible, have the same behavior as immiscible fluids at large capillary number, i.e., when the surface tension is negligible.

ACKNOWLEDGMENTS

The authors would like to gratefully acknowledge the CNES for financial support. C. D. Mitescu and E. Meiburg are also acknowledged for helpful comments.

[1] G. M. Homsy, "Viscous fingering in porous media," Annu. Rev. Fluid Mech. **19**, 271 (1987).
[2] D. D. Joseph, "Fluid dynamics of two miscible liquids with diffusion and gradient stresses," Eur. J. Mech. B/Fluids **9**, 565 (1990).
[3] B. Seijo, E. Fatal, and L. Roblot-Treudel, "Design of nanoparticles of less than 50 nm diameter: preparation, characterization and drug loading," Int. J. Pharm. **62**, 1 (1990).
[4] P. Garik, J. Hetrick, B. Orr, D. Barkey, and E. Ben-Jacob, "Interfacial cellular mixing and a conjecture on global deposit morphology," Phys. Rev. Lett. **66**, 1606 (1991).

[5]J. Friedel, ''Instabilité d'une interface en présence de potentiel chimique,'' J. Phys. (France) **44**, 25 (1980).
[6]A. Davaille, ''Two-layer thermal convection in miscible viscous fluids,'' J. Fluid Mech. **379**, 223 (1999).
[7]N. Ribe, ''Spouting and planform selection in the Rayleigh–Taylor instability of miscible viscous fluids,'' J. Fluid Mech. **377**, 27 (1998).
[8]D. Snyder and S. Tait, ''A flow-front instability in viscous gravity currents,'' J. Fluid Mech. **369**, 1 (1998).
[9]J. A. Whitehead, ''Fluid models of geophysical hotspots,'' Annu. Rev. Fluid Mech. **20**, 61 (1988).
[10]P. G. Saffman and G. I. Taylor, ''The penetration of a fluid into a porous medium or Hele–Shaw cell containing a more viscous liquid,'' J. Fluid Mech. **245**, 312 (1958).
[11]C. T. Tan and G. Homsy, ''Stability of miscible displacements in porous media: Rectilinear flow,'' Phys. Fluids **29**, 3549 (1986).
[12]J. C. Bacri, D. Salin, and Y. Yortsos, ''Analyse linéaire de la stabilité de l'écoulement de fluides miscibles en milieux poreux,'' C. R. Acad. Sci., **314**, 139 (1992).
[13]R. A. Wooding, ''Growth of fingers at an unstable diffusing interface in a porous medium or Hele–Shaw cell,'' J. Fluid Mech. **39**, 477 (1969).
[14]E. Lajeunesse, J. Martin, and N. Rakotomalala, ''3D instability of miscible displacements in a Hele–Shaw cell,'' Phys. Rev. Lett. **79**, 5254 (1997).
[15]L. Paterson, ''Fingering with miscible fluids in a Hele–Shaw cell,'' Phys. Fluids **28**, 26 (1985).
[16]D. Sharp, ''An overview on Rayleigh–Taylor instability,'' Physica D **12**, 3 (1984).
[17]S. Chandrasekhar, *Hydrodynamic and Hydromagnetic Stability* (Oxford University Press, Oxford, 1961).
[18]J. Fernandez, P. Kurowsky, P. Petitjeans, and E. Meiburg, ''Density-driven, unstable flows of miscible in a Hele–Shaw cell,'' J. Fluid Mech. (to be published).
[19]P. G. Saffman and G. I. Taylor, ''The penetration of a fluid into a porous medium or Hele–Shaw cell containing a more viscous liquid,'' Proc. R. Soc. London, Ser. A **245**, 312 (1958).
[20]F. Graf, E. Meiburg, and C. Hartel, ''Density-driven instabilities of miscible fluids in a Hele–Shaw cell: Linear stability analysis of the three-dimensional Stokes equations,'' J. Fluid Mech. (to be published).
[21]H. C. Brinkman, ''A calculation of the viscous force exerted by a flowing fluid on a dense swarm of particles,'' Appl. Sci. Res., Sect. A **1**, 27 (1947).
[22]P. Kurowski, C. Misbah, and S. Tchourkine, ''Gravitational instability of a fictitious front during mixing of miscible fluids,'' Europhys. Lett. **29**, 309 (1995).
[23]J. Fernandez, ''Instabilités gravitationnelles entre fluides miscibles,'' Thèse de doctorat de l'Université de Paris 6, 2001.
[24]H. R. Brown, ''Rayleigh–Taylor instability in a finite thickness layer of a viscous fluid,'' Phys. Fluids A **1**, 895 (1989).
[25]C. W. Park and G. M. Homsy, ''Two-phase displacement in Hele–Shaw cells: Theory,'' J. Fluid Mech. **139**, 291 (1984).
[26]A. Paterson, ''Wetting on heterogeneous surfaces: Imperfect Hele–Shaw cell,'' Ann. Phys. **21**, 337 (1996).
[27]T. Maxworthy, ''Experimental study of interface instability in a Hele–Shaw cell,'' Phys. Rev. A **39**, 5863 (1989).
[28]J. V. Maher, ''Development of viscous fingering patterns,'' Phys. Rev. Lett. **54**, 1498 (1985).
[29]M. R. Carey, S. W. Morris, and P. Kolodner, ''Convective fingering of an autocatalytic reaction front,'' Phys. Rev. E **53**, 6012 (1996).
[30]M. Bockmann and S. C. Muller, ''Growth rates of the buoyancy-driven instability of an autocatalytic reaction front in a narrow cell,'' Phys. Rev. Lett. **85**, 2506 (2000).